

Facial Expression Recognition with Controlled Privacy Preservation and Feature Compensation

Feng Xu^{1,2}, David Ahmedt-Aristizabal² Peterson Lars² Dadong Wang² Xun Li²

¹UNSW Sydney, ²CSIRO Data61, Australia

{feng.xu, david.ahmedtaristizabal, xun.li}@data61.csiro.au,

Abstract

Facial expression recognition (FER) systems raise significant privacy concerns due to the potential exposure of sensitive identity information. This paper presents a study on removing identity information while preserving FER capabilities. Drawing on the observation that low-frequency components predominantly contain identity information and high-frequency components capture expression, we propose a novel two-stream framework that applies privacy enhancement to each component separately. We introduce a controlled privacy enhancement mechanism to optimize performance and a feature compensator to enhance task-relevant features without compromising privacy. Furthermore, we propose a novel privacy-utility trade-off, providing a quantifiable measure of privacy preservation efficacy in closed-set FER tasks. Extensive experiments on the benchmark CREMA-D dataset demonstrate that our framework achieves 78.84% recognition accuracy with a privacy (facial identity) leakage ratio of only 2.01%, highlighting its potential for secure and reliable video-based FER applications. We encourage the readers to visit the project page: <https://fengxxu.github.io/ppfer/>.

1. Introduction

Facial Expression Recognition (FER) has been attracting growing attention due to its great value in various fields, such as medical diagnosis [3, 11, 52, 60], human-robot interaction [19, 33, 50] and driver fatigue detection [4, 17]. Protecting facial identity in these sensitive application areas is crucial, not only because it is required by law [1, 54], but also as an ethical and moral obligation to foster user trust and encourage participation. AI has revolutionized numerous industries with its transformative capabilities. However, it has yet to be widely adopted in human-related fields, primarily due to significant privacy concerns. As AI algorithms in these fields depend on extensive human data for training and optimization, securing sensitive data and limit-

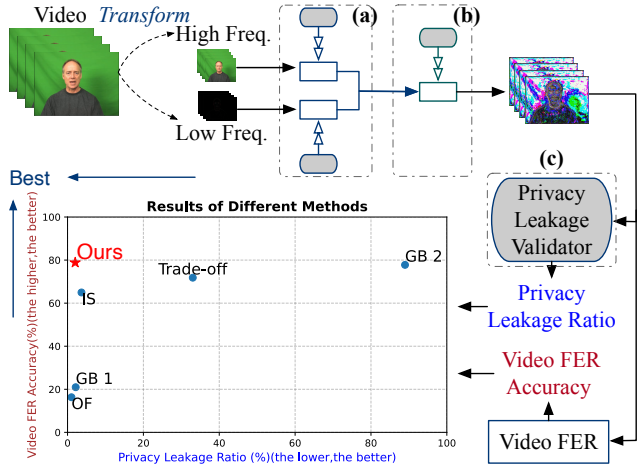


Figure 1. Our framework: (a). Controlled privacy-preservation in the high- and low-frequencies (Freq.) with (b). Controlled feature compensation and (c). Privacy leakage validation. The results show the performance of different privacy preservation approaches with video-based FER on privacy leakage ratio and video FER accuracy. GB 1 & 2, OF, Trade-off and IS are short for Gaussian Blurring 1 & 2, Optical Flow, Trade-off framework and Image Swapping, respectively.

ing access to authorized personnel only is essential.

Researchers have extensively studied privacy preservation for various utility tasks, from full-body behavior recognition to facial analysis. In this study, we focus on the latter task, where visual obfuscation techniques have been used to protect privacy. The preservation of facial privacy can be categorized into two scenarios [43]: *closed-set*, where the set of all possible identities in the observed data is known to the system, and *open-set*, where some identities in the observed data are not previously known to the system. Our work specifically addresses the closed-set scenario. We summarize existing approaches into four categories for both scenarios based on different methodologies employed. The first category of approaches [24, 56, 57, 59] distorts source data using techniques like blurring, pixelation, or noise addition to protect privacy, but these methods also disrupt fa-

cial features, compromising tasks such as facial biometrics recognition and FER. The second category focuses on face reconstruction [37]. While these two categories can partially preserve privacy, they remain vulnerable to recovery attacks [46]. The third category synthesizes new images, including face generation [6, 14] and face swapping [58], to preserve expressions or replace faces. Nevertheless, existing works on static images [34] highlight that facial expression features are not always transferred effectively. The last category is not explicitly designed for privacy protection but achieves it as a byproduct. For example, video data can be converted to optical flow [5], or infrared thermal images can be used to classify expressions in low-light settings [9]. While optical flow effectively protects privacy, it complicates downstream tasks. The infrared thermal approach performs well in low light but struggles with dataset domain shifts [13, 44]. Even though these works are not explicit about either open-set or closed-set scenarios, we observe a lack of mechanisms for evaluating privacy preservation for specific attributes, making quantitative comparisons difficult.

FER from video data presents unique challenges in balancing expression classification accuracy with privacy preservation. It requires removing facial identity features while retaining facial expression details for accurate recognition. Traditional methods [16, 51, 58] often struggle to effectively remove personal identity features without compromising facial expression dynamics, leaving privacy vulnerable to manual review. Moreover, utility task accuracy typically declines post-preservation. Although privacy enhancement is necessary, it inevitably degrades facial expression features, necessitating feature enhancement approaches to maintain performance. Despite prior efforts, there remains a lack of independent mechanisms to quantitatively assess privacy leakage.

In response to these challenges, our proposed framework, as shown in Figure 1, exploits the wavelet transform to remove personal identity features from the low-frequency and high-frequency components and separately removes the privacy identity features in low- and high-frequencies. The transformation is inspired by [21], which illustrates that the facial expression frequency band is higher than the facial identity frequency band. This has also been proven by subsequent works [8, 28]. In video clips, such as those depicting a transition from a neutral to a happy facial expression and back, personal identity features persist consistently across frames as low-frequency information, while the face expression dynamics, which constitute high-frequency information, will vary across frames. The frequency distinction, where facial expression information is carried in high frequency and identity information is mostly presented in low frequency, suggests a potential method to preserve expression while removing identity. Our framework adopts a dual

approach, removing facial identity from both low- and high-frequency components, as facial identity features may not reside exclusively in the low-frequency range. To optimize this, we introduce privacy enhancement controllers that adjust the privacy enhancer for each frequency by maximizing identity recognition loss. After privacy enhancement, the two frequency bands are fused, and frames are reconstructed via inverse transformation. This is followed by a feature compensator, inspired by [32], which enriches non-identity features, enhancing the fidelity of facial expression. In addition, we introduce a new mechanism that quantitatively assesses privacy preservation at the final step for performance validation. Concurrently, the utility task of FER has been implemented as a classifier at the final step operating on the reconstructed videos. The contributions of our paper are three-fold:

- We propose a new framework for privacy-preserved video-based facial expression recognition by using a dual approach, which separately removes existing identity privacy from high- and low-frequency components. This process is further enhanced by two dedicated privacy preservation controllers.
- We introduce a feature compensator that compensates the non-identity features to enhance the performance of the utility task (video-based FER in our case), ensuring robust performance even after privacy enhancement.
- We propose a novel mechanism that evaluates the effectiveness of privacy preservation by comparing the ground truth identity labels with the output produced from a facial identity classification network after removing identity information in the closed-set scenario. We believe that this mechanism can be extended to other privacy attributes for specific validation.

2. Related Work

Deidentification. To conceal the visual personal identity, PartialFace [38] hides visual information by pruning low-frequency components and applying random frequency components during training and inference to impede recovery. Building on PartialFace, MinusFace [39] further subtracts the features from original faces and their regenerated versions to produce protective face representations. While these methods effectively preserve privacy within the closed-set scenario, they are limited in face recognition tasks. Yoon et al. [61] protect privacy by altering biometric information to prevent recognition of biometric features. Techniques proposed by [10, 23] focus on deidentification, removing or replacing personal identifiers in biometric data. Additionally, Orekondy et al. [42] remove privacy-sensitive features from biometric images and construct visual redactions. Osorio-Roig et al. [43] evaluate

biometric privacy preservation approaches in both open-set and closed-set scenarios. These methods utilize various approaches to preserving privacy, but they fail to validate their privacy-enhanced images to demonstrate that the identity cannot be accurately recognized by computer vision models

Privacy-enhancement of Facial Expression A weighted supervised contrastive learning approach is used for privacy-enhancement in recognizing facial expression embedding from images [48]. Adversarial learning techniques are utilized by [40, 41] to train Convolutional Neural Networks (CNNs), preserving facial identity in images while ensuring high FER accuracy. Leibl et al. [29] subtract and blend facial identity from images, swapping faces and retaining the associated facial expression feature. Similarly, image synthesis is used to enhance privacy while preserving FER performance, as demonstrated in [14, 45]. IR-FacExNet [9] recognizes facial expressions from infrared thermal images, using a cosine annealing learning scheduler [35] to enhance overall performance. These works implement privacy-preserved FER based on images.

Privacy-enhancement of Soft-biometrics Wu et al. [57] propose an adversarial training framework to learn a privacy enhancement function that protects identity, gender, ethnicity, and other soft biometrics in closed-set scenarios. SPAct [16] builds upon this work by introducing a self-supervised privacy branch that addresses additional human-related privacy attributes in open-set scenario. Furthermore, TeD-SPAD [20] extends the SPAct framework to anomaly detection. These studies [16, 20, 36, 40, 41, 57] focus on trade-off frameworks that aim to balance privacy preservation with utility tasks, providing optimal solutions that reconcile these competing objectives.

Recognition of Facial Expression from Videos. Video-based FER has been extensively investigated, with recent works addressing challenges such as changes unrelated to facial expressions and overfitting in recognition models [2, 31]. Many studies [18, 27] utilize 3D CNNs to extract features from videos, while others, such as EC-STFL [25] combine Recurrent Neural Networks with CNNs for dynamic facial expression recognition. Advanced techniques, including intensity-aware loss with the global convolution-attention block [30], have been developed to further enhance recognition performance. M3DFEL [55] addresses short-term and long-term temporal relationships by generating 3D instances using 3D CNNs for feature extraction and dynamically aggregating long-term instances.

Feature Compensation. DAFE [15] enhances utility task-related features by reusing low-level image features derived from spatial details and pixel-wise features, leveraging channel-wise long-range relationships. SAFECount [62] employs location regression on the original images and integrates this with a similarity map to improve accuracy,

guided by a similarity metric. COSE [32] enhances images by learning from color shifts through over- and under-exposure of the original images. U-ViT [7] treats input patches as tokens, incorporating temporal, conditional, and noisy images to generate new outputs while utilizing long skip connections within its framework, significantly enhancing the performance of image diffusion models.

3. Method

In previous literature [16, 51, 58], we observe that most researchers treat privacy preservation and main utility tasks as a tangled problem, where their methodologies struggle to maintain the high performance of both tasks. In this research, we address such a dilemma by decoupling the two tasks in a way that two separate networks/mechanisms, namely the privacy preservation controller and feature compensator, have been designed and employed at the two tasks, respectively, thus achieving good performance for both.

3.1. Model Overview

The proposed framework consists of four key components, as illustrated in Figure 2: ① controlled privacy-preservation, ② controlled feature compensation, ③ privacy leakage validation (V_{pl}), and ④ the utility task (F_u), focusing on video-based FER. In the framework, F_{hpr} and C_{hpr} refer to the high-frequency privacy enhancer and its identity budget controller, respectively. Similarly, F_{lpr} and C_{lpr} denote the low-frequency privacy enhancer and its identity budget controller. F_{fc} and C_{fc} represent the non-identity feature compensator and its controller. The pre-trained controllers (C_{hpr} , C_{lpr} and C_{fc}) and the privacy leakage validator (V_{pl}) are frozen during each training process to maintain their integrity and effectiveness.

3.2. Controlled Privacy-Preservation

Previously, we established that while a person’s identity information persists across all frames in a video, facial expression undergoes dynamic changes. Thus, dividing the video into high- and low-frequency components allows for differential treatment of identity and expressive information. High-frequency components contain facial expressive information, whereas low-frequency components retain identity-related features. Because the identity-related features contained in the two are different, the removal of privacy at different frequencies should be different. Consequently, at the beginning of the framework, the original video is transformed into high- and low-frequency components (V_{ih} and V_{il}) to preserve privacy separately.

In our framework, controlled privacy-preservation, as illustrated in Algorithm 1, involves two main functions: an identity budget controller (C_{hpr} or C_{lpr}) and a privacy enhancer (F_{hpr} or F_{lpr}). The identity budget controller is implemented as a CNN-based classification model that is pre-

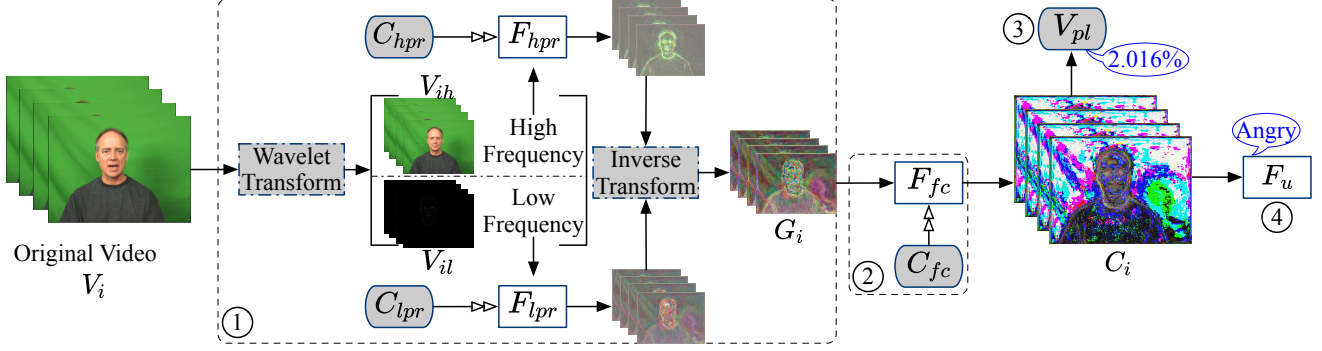


Figure 2. Illustration of our framework. ① Controlled privacy-preservation: the original video (V_i) is transformed into high- and low-frequency components (V_{ih} and V_{il}), followed by privacy enhancement, which includes a privacy enhancer (F_{hpr} and F_{lpr}) and its controller to strengthen privacy enhancement (C_{hpr} and C_{lpr}) for low- and high-frequency components respectively. The privacy-preserved high- and low-frequency frames are then combined and inverse-transformed into new video frames (G_i) for the next step. ② Controlled feature compensation involves a feature compensator (F_{fc}) and its controller (C_{fc}), which regulates the compensation of specific features. ③ Privacy leakage validation uses a privacy leakage validator (V_{pl}) to determine the proportion of identity features that can be recognized to measure the performance of privacy preservation. ④ Utility task (F_u) learns from the feature-rich video frames (C_i) on its main task, such as FER in our case. All grey components are frozen during training, and all controllers are not involved in inference.

Algorithm 1 Controlled privacy preservation training

Initialization: C_{hpr} , C_{lpr} , F_{hpr} and F_{lpr} load pre-trained weights

Input: A batch of training videos, facial expression labels and identity labels $(V_i, E_i, I_i) \in D$, where D is the training dataset with n batch of videos and $i \in \{1, \dots, n\}$

- 1: **for** $epoch = 1$ to N_1 **do**
- 2: Shuffle the training data
- 3: **for** $i = 1$ to n **do**
- 4: Wavelet transform V_i and get high- (V_{ih}) and low- (V_{il}) freq.;
- 5: C_{hpr} and C_{lpr} set as `.eval()`, F_{hpr} and F_{lpr} set as `.train()`;
- 6: # Forward pass:
- 7: High freq. output $y_{ih} := C_{hpr}(F_{hpr}(V_{ih}))$;
- 8: Low freq. output $y_{il} := C_{lpr}(F_{lpr}(V_{il}))$;
- 9: # Backward pass:
- 10: Update parameters of F_{hpr} and F_{lpr} via maximizing the cross-entropy losses of (y_{ih}, I_i) and (y_{il}, I_i) ;
- 11: **for** $i = 1$ to n **do** # Remove training set identity
- 12: $G_i :=$ inverse transform $F_{hpr}(V_{ih})$ and $F_{lpr}(V_{il})$;

Output: The privacy-preserved training videos G_i , $(G_i, E_i, I_i) \in D_G$, where D_G is the privacy-preserved training dataset.

trained on identity label datasets using cross-entropy loss. It classifies the identity of the person appearing in each video frame. On the other hand, the privacy enhancer, an encoder-decoder model, is pre-trained with $L1$ reconstruction loss

similar to [16]. In our framework, the initial parameters of C_{hpr} and C_{lpr} are identical, as are those of F_{hpr} and F_{lpr} . During training, C_{hpr} and C_{lpr} are frozen, and for each frequency, the transformed video serves as input for the privacy enhancer. The output of the privacy enhancer is then used as input for the identity budget controller, as shown in lines 7 and 8 of Algorithm 1. We compute the cross-entropy loss between the output of the identity budget controller and the identity labels, optimizing only the parameters of the privacy enhancer. The outputs from the high- and low-frequency privacy-preservation processes are then integrated and inverse transformed to reconstruct a video, G_i in Algorithm 1, which serves as the input for the subsequent components within the framework.

3.3. Controlled Feature Compensation

Algorithm 2 illustrates the controlled feature compensation training approach. The feature compensation module in our framework consists of two components: F_{fc} and C_{fc} . F_{fc} uses the U-ViT model [7], which integrates Vision Transformer (ViT) as the backbone for image generation with the diffusion model. This component enhances the utility-task related features for the privacy-preserved video frames. It intends to operate frame-by-frame to generate enhanced visual representations for downstream utility tasks while suppressing specific identity-related features. C_{fc} is a classification model employing ResNet50, pre-trained on a facial expression dataset collected in real-world conditions, using cross-entropy loss. This component learns from a wide variety of data collected in real-world conditions, thus ensuring that the guided feature compensation enhances the common facial expression features without being biased by specific identity-related features.

Algorithm 2 Controlled feature compensation training

Initialization: F_{fc} and C_{fc} load pre-trained weights

Input: $(G_i, E_i, I_i) \in D_G$ from Algorithm 1

- 1: **for** $epoch = 1$ to N_2 **do**
- 2: Shuffle the training data
- 3: **for** $i = 1$ to n **do**
- 4: C_{fc} sets as `.eval()`, F_{fc} sets as `.train()`;
- 5: # Forward pass:
- 6: $G_{ci} := F_{fc}(G_i)$;
- 7: $e_{gci} := C_{fc}(G_{ci})$;
- 8: # Backward pass:
- 9: Update parameters of F_{fc} via minimizing the cross-entropy loss (e_{gci}, E_i)
- 10: **for** $i = 1$ to n **do** # Compensate training set features
- 11: $C_i := F_{fc}(G_i)$;

Output: Feature compensated training set with facial expression labels $(C_i, E_i) \in D_G$

During the training process of F_{fc} , the pre-trained C_{fc} is frozen and provides feedback for F_{fc} . Optimization involves training F_{fc} using cross-entropy loss to guide the generation of facial expression feature-rich frames. This approach ensures that the feature compensation enhances the expressive content of privacy-preserved videos and generates feature-compensated video, C_i in Algorithm 2, while not affecting the privacy enhancement quality in the video.

3.4. Privacy Leakage Validation

As previously noted, we create the leakage validation mechanism based on identity recognition accuracy using a pre-trained classification network that registers all facial identities. Our privacy leakage validator V_{pl} uses ResNet50, pre-trained on the same dataset with identity labels as C_{hpr} and C_{lpr} , to recognize a random frame from the feature-compensated video. By maintaining consistency between C_{hpr} , C_{lpr} , and V_{pl} , we ensure that the privacy attribute being validated for leakage is the same one that was previously preserved. The V_{pl} measures privacy leakage by assessing the accuracy of recognizing facial identity features from privacy-preserved videos. A higher accuracy of V_{pl} indicates greater residual identity information in the video, thus higher privacy leakage. Consequently, the V_{pl} transfers its identity recognition accuracy into a measure of privacy leakage, providing a quantitative mechanism for comparing the performance of various privacy preservation approaches.

The privacy leakage validation process requires explicit privacy categories, such as identity, skin color, and gender. This enables an assessment of how effectively the privacy preservation method addresses specific privacy categories, regardless of the utility task.

3.5. Facial Expression Recognition

R3D [53] is selected as the network for the video-based FER. Previous works [22, 49] have demonstrated good performance in recognizing the expressions on our selected dataset. In our framework, the downstream task, F_u , does not affect the upstream tasks, including privacy preservation and feature compensation. Training F_u on V_i and C_i can demonstrate how our privacy preservation affects video-based FER by comparing the recognition accuracy of $F_u(V_i)$ and $F_u(C_i)$.

4. Experiments

4.1. Experimental Setup

Our framework operates in a closed-set scenario, requiring datasets that provide ground truth facial expression labels for classification and facial identity information for validating privacy protection. We selected the CREMA-D [12], which includes 7,442 video clips from 91 actors displaying six categories of facial expressions. For our experiments, we used 2,232 clips for testing (CREMA-D testing set) and the remaining clips for training (CREMA-D training set). The identity budget controllers and privacy leakage validator are pre-trained on the CREMA-D training set. The non-identity feature controller was pre-trained on 3,600 clips from the DFEW dataset [25], which contains 16,372 in-the-wild video clips from movies featuring 7 categories of facial expressions.

4.2. Implementation

As illustrated in Figure 2, our framework employs the wavelet transform to decompose the original video into high-frequency and low-frequency components. The assumption is that identity information is primarily contained in the low-frequency part, as the same individuals perform facial expressions throughout the video. Conversely, facial expressions representing dynamic changes are captured in the high-frequency part, except in the case of static images. To address privacy enhancement, our framework splits the process into two branches, each consisting of a privacy enhancer and an identity budget controller. Then, we follow a two-step training procedure. First, we train ResNet50 on the CREMA-D training set to recognize the identities of the 91 actors, serving as the identity budget controllers. These controllers achieve 100% accuracy on the CREMA-D testing set. Then we train the privacy enhancer, during which time its corresponding controller remains fixed throughout the training of privacy enhancer, making sure they effectively remove identity-related features. Both privacy enhancers use the U-Net [47] as the backbone and are pre-trained using L_1 reconstruction loss, similar to the anonymization function in SPAct [16]. Finally, the wavelet inverse transform is applied to the output of the high- and

low-frequency privacy enhancers to reconstruct the video frames.

In the controlled feature compensation, F_{fc} follows the U-ViT architecture [7] and uses the ‘‘ImageNet 256x256 (U-ViT-H/2)’’ pre-trained weights. The C_{fc} is pre-trained with cross-entropy loss on the DFEW dataset, using one random frame from each video. During training, C_{fc} remains frozen while F_{fc} is updated.

The V_{pl} utilizes ResNet50 with pre-trained parameters, the same as those used for C_{hpr} and C_{lpr} , for inference. Given that all frames within a feature-compensated video contain the same identity, a randomly selected frame from the video is used as input of V_{pl} . V_{pl} requires the ground truth privacy feature labels to validate prediction accuracy.

The utility task F_u employs the R3D, pre-trained on the Kinetics-400 [26] dataset and trained with cross-entropy loss, to perform video-based facial expression classification. The pre-training of C_{hpr} , C_{lpr} , C_{fc} , and V_{pl} , as well as the training of F_{hpr} , F_{lpr} , F_{fc} , and F_u , uses the CREMA-D training set or its generated set.

4.3. Baseline Comparison

To evaluate our framework, we first train F_u on the original dataset to check the performance of F_u , named ‘‘No Privacy Preservation’’ in Table 1. Then, we implement several baselines:

Distortion. We implement a Gaussian blur approach as the baseline to preserve identity. The formulation is $G(x, y) = \frac{1}{2\pi\sigma^2} e^{-\frac{x^2+y^2}{2\sigma^2}}$, where x and y are the horizontal and vertical distances from the center, and σ is the standard deviation. As σ controls the degree of blurring, we implement two baselines aiming to align with our performance of either privacy enhancement or utility task to compare the trade-off. Firstly, we set the degree of privacy leakage (2.150%) after Gaussian blur to be closed to our approach (2.016%), named ‘‘Gaussian Blur 1’’ in Table 1, and we observe the performance of F_u . Secondly, we adjust the Gaussian blur, named ‘‘Gaussian Blur 2’’ in Table 1, so that the accuracy (77.778%) of the utility task reaches the same level as our results (78.843%), and then we observe the privacy leakage ratio.

Privacy-enhancement via adversarial learning. We also implement SPAct [16], a bi-objective optimization framework, a state-of-the-art self-supervised privacy enhancement approach building upon an adversarial learning framework [57], and we name it as ‘‘Trade-off Framework’’ in Table 1.

De-identification. The approach involves transforming the image or video data into another modality, such as converting video to optical flow. We select a state-of-the-art framework, VideoFlow [51]), as the de-identification baseline, named as ‘‘optical flow’’ in Table 1.

Image swapping. This approach aims to demonstrate that

Approach	↓ PLR	↑ ACC
No Privacy Preservation	100%	87.201%
Gaussian Blur 1	2.150%	20.968%
Gaussian Blur 2	88.978%	77.778%
Trade-off Framework	33.020%	71.827%
Optical Flow	1.030%	16.308%
Image Swapping	3.674%	64.964%
Ours	2.016%	78.843%

Table 1. Privacy Leakage Ratio (PLR) and Utility Task Accuracy (ACC) of different privacy-preserving approaches and without privacy preservation.

Exp	Ang	Dis	Fea	Hap	Neu	Sad	↑ Avg
NPP	91.7%	98.8%	80.3%	98.3%	84.9%	80.8%	87.2%
Ours	93.6%	81.2%	80.0%	96.7%	80.7%	40.9%	78.8%

Table 2. Recognition accuracy of FER for videos on each facial expression after applying our proposed methods. NPP stands for no privacy preservation.

face swapping could preserve facial landmarks while hiding personal identity. We utilize a state-of-the-art approach [58] that utilizes a face not in the dataset to swap all faces appearing in the CREMA-D testing set. V_{pl} and F_u perform the same tasks as in our framework on the output of face swapping. The results are shown as ‘‘Image Swapping’’ in Table 1.

4.4. Evaluation

The experimental results are evaluated using our proposed privacy leakage evaluation mechanism and a utility task evaluation metric: privacy leakage ratio from V_{pl} , indicating the ability of privacy-preservation, and video-based FER accuracy from F_u , indicating the performance of our framework. As illustrated in Section 4.1, the dataset contains 91 actor identities. The ideal ratio of the V_{pl} result should be close to $\frac{1}{91}$, or approximately 1.099%. Similarly, the accuracy of the privacy-preserved video-based FER task should ideally be close to the accuracy of the standard video-based FER task.

Table 1 lists the privacy leakage ratio and utility task accuracy. The ‘‘No privacy preservation’’ row represents the F_u -only task, illustrating the performance upper bound for F_u without any privacy preservation. When the privacy leakage ratio of Gaussian Blur 1 is 2.150% on the CREMA-D test set, which is close to but higher than our framework’s privacy leakage ratio, the video-based FER accuracy is 20.968%. Conversely, When the utility task accuracy of Gaussian Blur 2 is 77.778%, which is close to but lower than our framework’s utility task accuracy, the privacy leakage ratio reaches 88.978%. Table 2 shows the recognition accuracy of each expression before and after privacy enhancement. The results of the two experimental approaches demonstrate the difficulty in balancing privacy preservation

Approach	↓ SSIM	↓ PSNR	↓ PLR
Gaussian Blur 1	0.94	31.14	72.45%
Gaussian Blur 2	0.96	32.54	94.58%
Trade-off Framework	0.57	19.97	46.19%
Optical Flow	0.40	9.59	5.91%
Image Swapping	0.50	15.46	41.91%
Ours	0.41	10.18	5.65%

Table 3. Quantitative results of the threat model for our method and baselines on CREMA-D testing set.

and utility tasks using blurring techniques.

To benchmark our framework further, we used three state-of-the-art privacy-preserving approaches and implemented them on the CREMA-D dataset. The trade-off framework ensures relatively high recognition accuracy; however, the facial identity in privacy-preserved videos can still be classified with relatively high accuracy. The privacy-preserving effect of the optical flow and image swapping is a byproduct. The optical flow approach achieves the lowest privacy leakage ratio but also obtains the lowest FER accuracy. In the image swapping experiment, an author’s face replaces all faces in the test set. The results also support the conclusion from [34] that swapping cannot adequately transfer the expression features to the swapped faces.

4.5. Threat Model

In our framework, we consider a white-box attacker who can access all details except for the controllers C_{hpr} , C_{lpr} and C_{fc} which are removed during deployment. The attacker can use the outputs from our training set alongside the original training set to train a recovery model. Following recent approaches [24, 38, 39], we employ a full-scale U-Net [47] as the recovery model. Using the CREMA-D training set, the outputs of our framework, as well as those from other baselines, serve as training inputs for the U-Net. We train six U-Nets, one for ours and the other five for baselines, using L_1 reconstruction loss in conjunction with the original videos. For quantitative comparison, we use structural similarity (SSIM), peak signal-to-noise ratio (PSNR), and our proposed PLR for privacy preservation evaluation. The results are shown in Table 3. It shows that our method, together with optical flow, significantly outperforms the other five methods of privacy preservation against recovery attacks. However, the optical flow fails on the utility task, while our method demonstrates the highest performance on utility task, as shown in Table 1.

4.6. Ablation Study

Table 4 shows the ablation study results, focusing on the components of controlled privacy preservation and controlled feature compensation, labeled as ① and ② in Figure 2. Figure 3 and Figure 4 illustrate the details of each ablation study task.

Task 1 removes the wavelet transformation and inverse

Task No.	Components					PLR	ACC
	T&IT. ^a	PE ^b	IBC. ^c	FC. ^d	FCC. ^e		
1	✗	✓	✓	✓	✓	12.993%	73.028%
2	✗	✓	✗	✓	✓	32.975%	72.429%
3	✗	✓	✓	✗	✗	12.903%	54.487%
4	✓	✓	✓	✓	✗	2.106%	61.187%
5	✓	✓	✓	✗	✗	2.061%	48.656%
6	✓	✓	✗	✗	✗	31.989%	68.831%

- ^a Transformation and Inverse Transformation;
- ^b Privacy Enhancers;
- ^c Identity Budget Controller;
- ^d Feature Compensator;
- ^e Feature Compensator Controller.

Table 4. Ablation Study Overview.

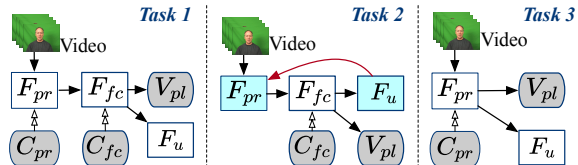


Figure 3. F_{pr} and C_{pr} denote the privacy enhancer and its controller. They work on the original video. The privacy enhancer and identity budget controller (in purple) share identical architectures and weights with F_{hpr} and C_{hpr} , respectively. In Task 2, the controller-free privacy enhancer is trained while updating F_u .

transformation steps in the controlled privacy preservation process. Without the separated privacy enhancer on high- and low-frequency components, the PLR increased. This demonstrates the importance of handling high- and low-frequency information separately to ensure effective privacy preservation.

Task 2 further removes the identity budget controller, utilizing a bi-optimization approach in its absence. The results show a dramatic increase in privacy leakage, highlighting the crucial role of the identity budget controller in maintaining privacy while performing FER.

Task 3 removes the controlled feature compensation. Unlike Task 1, it maintains the controlled privacy preservation using ResNet50 initialized with the same parameters as C_{hpr} and C_{lpr} , and a U-Net initialized with the same parameters as F_{hpr} and F_{lpr} . The absence of controlled feature compensation affects the balance between privacy preservation and utility task performance.

Task 4 removes C_{fc} , and F_{fc} is trained with mean squared error loss. The privacy leakage ratio remains at a similar level, with 46 identities correctly predicted, compared to 45 in our full framework. Without C_{fc} , the non-identity feature compensation is not as effective as required for the video-based FER.

Task 5 removes both C_{fc} and F_{fc} , eliminating the en-

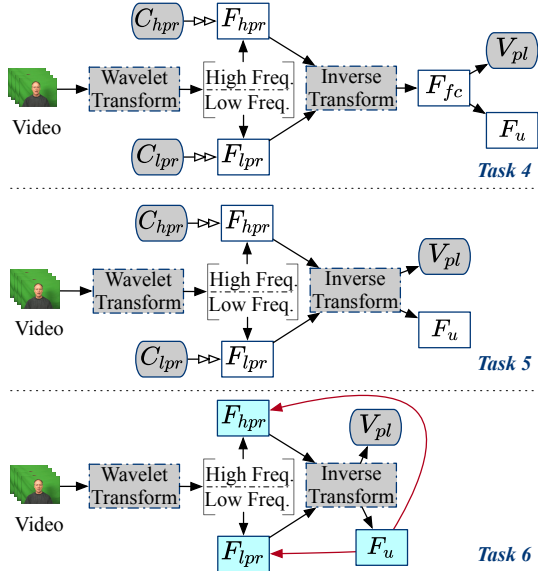


Figure 4. The structure of Tasks 4, 5 and 6. In Task 6, the parameters of controller-free F_{hpr} and F_{lpr} are updated while training F_u .

tire controlled feature compensation component. This corresponds to removing ② from the framework in Figure 2. The F_u is trained directly on the privacy-preserved videos from ①. The video-based FER performs sub-optimally on these privacy-preserved videos due to insufficient non-identity features.

Task 6 further removes the identity budget controller from Task 5. F_{hpr} , F_{lpr} and F_u are trained as a whole. The transform, being a function with only hyperparameters, does not participate in the training process. The parameter update process is indicated by the red arrow. Despite the transformations applied, the absence of an identity budget controller results in sub-optimal performance for privacy enhancement.

The results of Tasks 1, 2, 3 and the full framework demonstrate that utilizing high- and low-frequencies privacy enhancement can effectively remove the identity information from the video. The results of Tasks 4 and 5 highlight the importance of the controlled feature compensation in improving the performance of video-based FER. Our proposed controlled feature compensation effectively enriches the facial expression features, counteracting their potential loss during privacy enhancement. Task 6 and our main results demonstrate that the privacy leakage validation mechanism can effectively evaluate privacy preservation approaches based on specific privacy attributes, such as the facial identity feature in our experiment.

In addition, by observing the results of Tasks 2, 3, 5, and 6 for the privacy-preserving video-based FER task, we conclude that our proposed transformation- and control-based privacy preservation approach can effectively remove spe-

cific privacy features. The results from bi-optimization approaches, specifically, Tasks 2 and 6 in Table 4 and the Trade-off Framework in Table 1, indicate that the bi-optimization approaches require further work to adapt to privacy-preserved video-based FER. Our framework decouples the privacy-preservation and utility tasks, connecting them via the controlled feature compensation, thereby enhancing the performance of both parts. From the results of Tasks 1 and 4 or 2 and 4, it is evident that features need to be enhanced under control rather than randomly. Even after transformation, the facial identity and expression features cannot be completely separated, making it impossible to achieve the ideal utility task accuracy of 87.201% as seen with no privacy preservation in Table 1.

4.7. Limitation and Future work

Our framework has the following limitations. Firstly, the dataset must contain privacy labels, which are used to control the privacy enhancer during training. As a result, our framework cannot adapt to in-the-wild datasets without privacy labels. However, we have demonstrated the effectiveness and necessity of the controller for privacy preservation in Section 4.6. In future research, we will further improve the framework to adapt to open-set scenarios and handle in-the-wild datasets. Secondly, our privacy preservation focuses solely on facial identity attributes. There is still room to explore and adapt our framework for other utility tasks, such as pose estimation. Thirdly, our utility task selects a basic video-analyzing neural network for video-based FER. A state-of-the-art video FER model could potentially further improve utility task accuracy. It is, however, not our main goal in this research. A simple network, such as R3D used in this work, is sufficient to demonstrate the impact of our proposed privacy-preserving process on video-based FER tasks while remaining robust to the recovery attack. The small difference in accuracy between the privacy-preserving and non-privacy-preserving scenarios demonstrates the superiority of our framework.

5. Conclusion

We propose a novel privacy-preserved video-based FER framework that removes facial identity features from both low-frequency and high-frequency components via a wavelet transform, followed by an inverse transform. The framework compensates features in the inverse-transformed videos to generate feature-rich content for downstream utility tasks. Additionally, we introduce the privacy leakage ratio in the closed-set scenario, a mechanism for evaluating the privacy preservation approach. Our extensive experiments demonstrate that our framework achieves competitive results with a low privacy leakage ratio and high performance in video-based FER, explaining the reasons for these results.

References

- [1] Accountability Act. Health insurance portability and accountability act of 1996. *Public law*, 104:191, 1996. **1**
- [2] R Rashmi Adyapady and B Annappa. A comprehensive review of facial expression recognition techniques. *Multimedia Systems*, 29(1):73–103, 2023. **3**
- [3] David Ahmedt-Aristizabal, Clinton Fookes, Kien Nguyen, Simon Denman, Sridha Sridharan, and Sasha Dionisio. Deep facial analysis: A new phase i epilepsy evaluation using computer vision. *Epilepsy & Behavior*, 82:17–24, 2018. **1**
- [4] Alexandra Branzan Albu, Ben Widsten, Tiange Wang, Julie Lan, and Jordana Mah. A computer vision-based system for real-time detection of sleep onset in fatigued drivers. In *2008 IEEE intelligent vehicles symposium*, pages 25–30. IEEE, 2008. **1**
- [5] Benjamin Allaert, Isaac Ronald Ward, Ioan Marius Bilasco, Chabane Djeraba, and Mohammed Bennamoun. A comparative study on optical flow for facial expression analysis. *Neurocomputing*, 500:434–448, 2022. **2**
- [6] TS Ashwin and Ramkumar Rajendran. Preserving privacy of face and facial expression in computer vision data collected in learning environments. In *International Conference on Artificial Intelligence in Education*, pages 561–567. Springer, 2023. **2**
- [7] Fan Bao, Shen Nie, Kaiwen Xue, Yue Cao, Chongxuan Li, Hang Su, and Jun Zhu. All are worth words: A vit backbone for diffusion models. In *Proceedings of the IEEE/CVF conference on computer vision and pattern recognition*, pages 22669–22679, 2023. **3, 4, 6**
- [8] Sarah Bate and Rachel Bennetts. The independence of expression and identity in face-processing: Evidence from neuropsychological case studies. *Frontiers in psychology*, 6:770, 2015. **2**
- [9] Ankan Bhattacharyya, Somnath Chatterjee, Shibaprasad Sen, Aleksandr Sinitca, Dmitrii Kaplun, and Ram Sarkar. A deep learning model for classifying human facial expressions from infrared thermal images. *Scientific reports*, 11(1):20696, 2021. **2, 3**
- [10] Karla Brkic, Ivan Sikiric, Tomislav Hrkac, and Zoran Kalafatic. I know that person: Generative full body and face de-identification of people in images. In *2017 IEEE Conference on Computer Vision and Pattern Recognition Workshops (CVPRW)*, pages 1319–1328. IEEE, 2017. **2**
- [11] Sam Cantrill, David Ahmedt-Aristizabal, Lars Petersson, Hanna Suominen, and Mohammad Ali Armin. Orientation-conditioned facial texture mapping for video-based facial remote photoplethysmography estimation. In *Proceedings of the IEEE/CVF Conference on Computer Vision and Pattern Recognition*, pages 354–363, 2024. **1**
- [12] Houwei Cao, David G Cooper, Michael K Keutmann, Ruben C Gur, Ani Nenkova, and Ragini Verma. Crema-d: Crowd-sourced emotional multimodal actors dataset. *IEEE transactions on affective computing*, 5(4):377–390, 2014. **5**
- [13] Somnath Chatterjee, Debyarati Saha, Shibaprasad Sen, Diego Oliva, and Ram Sarkar. Moth-flame optimization based deep feature selection for facial expression recognition using thermal images. *Multimedia Tools and Applications*, 83(4):11299–11322, 2024. **2**
- [14] Jiawei Chen, Janusz Konrad, and Prakash Ishwar. Vgan-based image representation learning for privacy-preserving facial expression recognition. In *Proceedings of the IEEE conference on computer vision and pattern recognition workshops*, pages 1570–1579, 2018. **2, 3**
- [15] Ming Chen, Yingjie Qin, Lizhe Qi, and Yunquan Sun. Improving fashion landmark detection by dual attention feature enhancement. In *Proceedings of the IEEE/CVF International Conference on Computer Vision Workshops*, pages 0–0, 2019. **3**
- [16] Ishan Rajendrakumar Dave, Chen Chen, and Mubarak Shah. Spact: Self-supervised privacy preservation for action recognition. In *Proceedings of the IEEE/CVF Conference on Computer Vision and Pattern Recognition*, pages 20164–20173, 2022. **2, 3, 4, 5, 6**
- [17] Guanglong Du, Tao Li, Chunquan Li, Peter X Liu, and Di Li. Vision-based fatigue driving recognition method integrating heart rate and facial features. *IEEE transactions on intelligent transportation systems*, 22(5):3089–3100, 2020. **1**
- [18] Yin Fan, Xiangju Lu, Dian Li, and Yuanliu Liu. Video-based emotion recognition using cnn-rnn and c3d hybrid networks. In *Proceedings of the 18th ACM international conference on multimodal interaction*, pages 445–450, 2016. **3**
- [19] Diego R Faria, Mario Vieira, Fernanda CC Faria, and Cristiano Premebida. Affective facial expressions recognition for human-robot interaction. In *2017 26th IEEE international symposium on robot and human interactive communication (RO-MAN)*, pages 805–810. IEEE, 2017. **1**
- [20] Joseph Fiorese, Ishan Rajendrakumar Dave, and Mubarak Shah. Ted-spac: Temporal distinctiveness for self-supervised privacy-preservation for video anomaly detection. In *Proceedings of the IEEE/CVF International Conference on Computer Vision*, pages 13598–13609, 2023. **3**
- [21] Xiaoqing Gao and Daphne Maurer. A comparison of spatial frequency tuning for the recognition of facial identity and facial expressions in adults and children. *Vision Research*, 51(5):508–519, 2011. **2**
- [22] Lucas Goncalves, Seong-Gyun Leem, Wei-Cheng Lin, Berrak Sisman, and Carlos Busso. Versatile audio-visual learning for handling single and multi modalities in emotion regression and classification tasks. *arXiv preprint arXiv:2305.07216*, 2023. **5**
- [23] Ralph Gross, Latanya Sweeney, Fernando de la Torre, and Simon Baker. Semi-supervised learning of multi-factor models for face de-identification. In *2008 IEEE Conference on Computer Vision and Pattern Recognition*, pages 1–8, 2008. **2**
- [24] Jiazhen Ji, Huan Wang, Yuge Huang, Jiexiang Wu, Xingkun Xu, Shouhong Ding, Shengchuan Zhang, Liujuan Cao, and Rongrong Ji. Privacy-preserving face recognition with learnable privacy budgets in frequency domain. In *European Conference on Computer Vision*, pages 475–491. Springer, 2022. **1, 7**
- [25] Xingxun Jiang, Yuan Zong, Wenming Zheng, Chuangao Tang, Wanchuang Xia, Cheng Lu, and Jiateng Liu. Dfew: A

- large-scale database for recognizing dynamic facial expressions in the wild. In *Proceedings of the 28th ACM International Conference on Multimedia*, pages 2881–2889, 2020. 3, 5
- [26] Will Kay, Joao Carreira, Karen Simonyan, Brian Zhang, Chloe Hillier, Sudheendra Vijayanarasimhan, Fabio Viola, Tim Green, Trevor Back, Paul Natsev, et al. The kinetics human action video dataset. *arXiv preprint arXiv:1705.06950*, 2017. 6
- [27] Jean Kossaifi, Antoine Toisoul, Adrian Bulat, Yannis Panagakis, Timothy M Hospedales, and Maja Pantic. Factorized higher-order cnns with an application to spatio-temporal emotion estimation. In *Proceedings of the IEEE/CVF conference on computer vision and pattern recognition*, pages 6060–6069, 2020. 3
- [28] Devpriya Kumar and Narayanan Srinivasan. Emotion perception is mediated by spatial frequency content. *Emotion*, 11(5):1144, 2011. 2
- [29] Andreas Leibl, Andreas Meißner, Stefan Altmann, Andreas Attenberger, and Helmut Mayer. De-identifying face image datasets while retaining facial expressions. In *2023 IEEE International Joint Conference on Biometrics (IJCB)*, pages 1–10. IEEE, 2023. 3
- [30] Hanting Li, Hongjing Niu, Zhaoqing Zhu, and Feng Zhao. Intensity-aware loss for dynamic facial expression recognition in the wild. In *Proceedings of the AAAI Conference on Artificial Intelligence*, volume 37, pages 67–75, 2023. 3
- [31] Shan Li and Weihong Deng. Deep facial expression recognition: A survey. *IEEE transactions on affective computing*, 13(3):1195–1215, 2020. 3
- [32] Yiyu Li, Ke Xu, Gerhard Petrus Hancke, and Rynson WH Lau. Color shift estimation-and-correction for image enhancement. In *Proceedings of the IEEE/CVF Conference on Computer Vision and Pattern Recognition*, pages 25389–25398, 2024. 2, 3
- [33] Zhentao Liu, Min Wu, Weihua Cao, Luefeng Chen, Jianping Xu, Ri Zhang, Mengtian Zhou, and Junwei Mao. A facial expression emotion recognition based human-robot interaction system. *IEEE CAA J. Autom. Sinica*, 4(4):668–676, 2017. 1
- [34] Juan-Miguel López-Gil, Rosa Gil, and Roberto García. Do deepfakes adequately display emotions? a study on deepfake facial emotion expression. *Computational intelligence and neuroscience*, 2022(1):1332122, 2022. 2, 7
- [35] Ilya Loshchilov and Frank Hutter. Sgdr: Stochastic gradient descent with warm restarts. *arXiv preprint arXiv:1608.03983*, 2016. 3
- [36] Yin-Yin Low, Angeline Tanvy, Raphaël C-W Phan, and Xiaojun Chang. Adverfacial: Privacy-preserving universal adversarial perturbation against facial micro-expression leakages. In *ICASSP 2022-2022 IEEE International Conference on Acoustics, Speech and Signal Processing (ICASSP)*, pages 2754–2758. IEEE, 2022. 3
- [37] Guangan Mai, Kai Cao, Pong C Yuen, and Anil K Jain. On the reconstruction of face images from deep face templates. *IEEE Trans Pattern Anal Mach Intell*, 41(5):1188–1202, 2018. 2
- [38] Yuxi Mi, Yuge Huang, Jiazhen Ji, Minyi Zhao, Jiaxiang Wu, Xingkun Xu, Shouhong Ding, and Shuigeng Zhou. Privacy-preserving face recognition using random frequency components. In *Proceedings of the IEEE/CVF International Conference on Computer Vision*, pages 19673–19684, 2023. 2, 7
- [39] Yuxi Mi, Zhizhou Zhong, Yuge Huang, Jiazhen Ji, Jianqing Xu, Jun Wang, Shaoming Wang, Shouhong Ding, and Shuigeng Zhou. Privacy-preserving face recognition using trainable feature subtraction. In *Proceedings of the IEEE/CVF Conference on Computer Vision and Pattern Recognition*, pages 297–307, 2024. 2, 7
- [40] Vansh Narula, Theodora Chaspari, et al. An adversarial learning framework for preserving users’ anonymity in face-based emotion recognition. *arXiv preprint arXiv:2001.06103*, 2020. 3
- [41] Vansh Narula, Kexin Feng, and Theodora Chaspari. Preserving privacy in image-based emotion recognition through user anonymization. In *Proceedings of the 2020 International Conference on Multimodal Interaction*, pages 452–460, 2020. 3
- [42] Tribhuvanesh Orekondy, Mario Fritz, and Bernt Schiele. Connecting pixels to privacy and utility: Automatic redaction of private information in images. In *Proceedings of the IEEE Conference on Computer Vision and Pattern Recognition*, pages 8466–8475, 2018. 2
- [43] Dailé Osorio-Roig, Christian Rathgeb, Pawel Drozdowski, and Christoph Busch. Stable hash generation for efficient privacy-preserving face identification. *IEEE Transactions on Biometrics, Behavior, and Identity Science*, 4(3):333–348, 2021. 1, 2
- [44] S Babu Rajendra Prasad and B Sai Chandana. Mobilenetv3: a deep learning technique for human face expressions identification. *International journal of information technology*, 15(6):3229–3243, 2023. 2
- [45] Yogachandran Rahulamathavan and Muttukrishnan Rajarajan. Efficient privacy-preserving facial expression classification. *IEEE Transactions on Dependable and Secure Computing*, 14(3):326–338, 2015. 3
- [46] Anton Razzhigaev, Klim Kireev, Edgar Kaziakhmedov, Nurislam Tursynbek, and Aleksandr Petiushko. Black-box face recovery from identity features. In *Computer Vision—ECCV 2020 Workshops: Glasgow, UK, August 23–28, 2020, Proceedings, Part V 16*, pages 462–475. Springer, 2020. 2
- [47] Olaf Ronneberger, Philipp Fischer, and Thomas Brox. U-net: Convolutional networks for biomedical image segmentation. In *Medical image computing and computer-assisted intervention—MICCAI 2015: 18th international conference, Munich, Germany, October 5-9, 2015, proceedings, part III 18*, pages 234–241. Springer, 2015. 5, 7
- [48] Felix Rosberg and Cristofer Englund. Comparing facial expressions for face swapping evaluation with supervised contrastive representation learning. In *2021 16th IEEE International Conference on Automatic Face and Gesture Recognition (FG 2021)*, pages 01–05. IEEE, 2021. 3
- [49] Elena Ryumina, Denis Dresvyanskiy, and Alexey Karpov. In search of a robust facial expressions recognition model:

- A large-scale visual cross-corpus study. *Neurocomputing*, 514:435–450, 2022. 5
- [50] Gabriel J Serfaty, Virgil O Barnard, and Joseph P Salisbury. Generative facial expressions and eye gaze behavior from prompts for multi-human-robot interaction. In *Adjunct Proceedings of the 36th Annual ACM Symposium on User Interface Software and Technology*, pages 1–3, 2023. 1
- [51] Xiaoyu Shi, Zhaoyang Huang, Weikang Bian, Dasong Li, Manyuan Zhang, Ka Chun Cheung, Simon See, Hongwei Qin, Jifeng Dai, and Hongsheng Li. Videoflow: Exploiting temporal cues for multi-frame optical flow estimation. In *Proceedings of the IEEE/CVF International Conference on Computer Vision*, pages 12469–12480, 2023. 2, 3, 6
- [52] Saurabh Sonkusare, David Ahmedt-Aristizabal, Matthew J Aburn, Vinh Thai Nguyen, Tianji Pang, Sascha Frydman, Simon Denman, Clinton Fookes, Michael Breakspear, and Christine C Guo. Detecting changes in facial temperature induced by a sudden auditory stimulus based on deep learning-assisted face tracking. *Scientific reports*, 9(1):4729, 2019. 1
- [53] Du Tran, Heng Wang, Lorenzo Torresani, Jamie Ray, Yann LeCun, and Manohar Paluri. A closer look at spatiotemporal convolutions for action recognition. In *Proceedings of the IEEE conference on Computer Vision and Pattern Recognition*, pages 6450–6459, 2018. 5
- [54] Paul Voigt and Axel Von dem Bussche. The eu general data protection regulation (gdpr). *A Practical Guide, 1st Ed., Cham: Springer International Publishing*, 10(3152676):10–5555, 2017. 1
- [55] Hanyang Wang, Bo Li, Shuang Wu, Siyuan Shen, Feng Liu, Shouhong Ding, and Aimin Zhou. Rethinking the learning paradigm for dynamic facial expression recognition. In *Proceedings of the IEEE/CVF conference on computer vision and pattern recognition*, pages 17958–17968, 2023. 3
- [56] Yinggui Wang, Jian Liu, Man Luo, Le Yang, and Li Wang. Privacy-preserving face recognition in the frequency domain. In *Proceedings of the AAAI Conference on Artificial Intelligence*, volume 36, pages 2558–2566, 2022. 1
- [57] Zhenyu Wu, Haotao Wang, Zhaowen Wang, Hailin Jin, and Zhangyang Wang. Privacy-preserving deep action recognition: An adversarial learning framework and a new dataset. *IEEE Transactions on Pattern Analysis and Machine Intelligence*, 44(4):2126–2139, 2020. 1, 3, 6
- [58] Zhiliang Xu, Zhibin Hong, Changxing Ding, Zhen Zhu, Junyu Han, Jingtuo Liu, and Errui Ding. Mobilefaceswap: A lightweight framework for video face swapping. In *Proceedings of the AAAI Conference on Artificial Intelligence*, volume 36, pages 2973–2981, 2022. 2, 3, 6
- [59] Yan Yan, Zizhao Zhang, Si Chen, and Hanzi Wang. Low-resolution facial expression recognition: A filter learning perspective. *Signal Processing*, 169:107370, 2020. 1
- [60] Minqiang Yang, Yu Ma, Zhenyu Liu, Hanshu Cai, Xiping Hu, and Bin Hu. Undisturbed mental state assessment in the 5g era: a case study of depression detection based on facial expressions. *IEEE Wireless Communications*, 28(3):46–53, 2021. 1
- [61] Soweon Yoon, Jianjiang Feng, and Anil K Jain. Altered fingerprints: Analysis and detection. *IEEE transactions on pattern analysis and machine intelligence*, 34(3):451–464, 2012. 2
- [62] Zhiyuan You, Kai Yang, Wenhan Luo, Xin Lu, Lei Cui, and Xinyi Le. Few-shot object counting with similarity-aware feature enhancement. In *Proceedings of the IEEE/CVF Winter Conference on Applications of Computer Vision*, pages 6315–6324, 2023. 3